Nature Environment and Pollution Technology
An International Quarterly Scientific Journal

p-ISSN: 0972-6268
(Print copies up to 2016)
e-ISSN: 2395-3454

Vol. 21 | No. 2 | pp. 829-836 | 2022

Original Research Paper

https://doi.org/10.46488/NEPT.2022.v21i02.047

Open Access Journal

The Drawing Characteristics and Critical Length of Single Polypropylene Fiber in Vegetation Concrete

Daxiang Liu *(**), Deyu Liu *, Baohua Zhang*, Bin Zhong*, Yueshu Yang*†, Jiangang Chen**, Yu Ding****, Zhenyao Xia**** and Wennian Xu****

*Key Laboratory of Disaster Prevention and Mitigation (China Three Gorges University), Hubei Province, Yichang 443002, China

**Key Laboratory of Mountain Hazards and Surface Processes, Institute of Mountain Hazards and Environment, Chinese Academy of Sciences, Chengdu 610041, China

***Fujian Yongtai Mintou Pumped Storage Co. Ltd., Fuzhou 350799, China

****Key Laboratory of Geological Hazards on Three Gorges Reservoir Area (China Three Gorges University), Ministry of Education, Yichang 443002, China

†Corresponding author: Yueshu Yang; michael_lewandowski@foxmail.com

Nat. Env. & Poll. Tech.
Website: www.neptjournal.com

Received: 24-06-2021
Revised: 05-08-2021
Accepted: 27-08-2021

Key Words:
Polypropylene fiber
Vegetation concrete
Drawing characteristics
Critical length
Empirical formula

ABSTRACT

Fiber-reinforced technology is an important method to improve the stability and durability of growing basis material. To evaluate the factors affecting the interfacial strength properties of polypropylene fiber reinforced vegetation concrete, single polypropylene fiber drawing tests were conducted by using a modified apparatus. The mechanical interaction behavior between vegetation concrete and polypropylene fiber was discussed by using a polarizing microscope. The results indicate that the drawing curves between polypropylene fiber and vegetation concrete show a typical multi-peak characteristic. And the interfacial shear strength is the minimum at the optimum water content (20%) in the 1d sample. It should be noted that both interfacial peak strength (IPS) and interfacial residual strength (IRS) increase with the increase of dry density and curing time for vegetation concrete. Then through multiple linear regression analysis, the empirical formula of critical fiber length in reinforced vegetation concrete is obtained, which can improve the engineering durability of vegetation concrete in harsh conditions.

INTRODUCTION

Vegetation concrete ecological protection technology, the theory of which refers to both civil engineering and ecology fields with the characteristics of high construction efficiency, low cost, and good engineering durability compared with other slopes ecological protection technology, is more suitable for the ecological protection of high steep rock slope which is more than 45° (Xia et al. 2011, Xu et al. 2019). And the vegetation concrete not only has a certain high strength and corrosion resistance characteristics but also has a porous structure similar to natural soil, thus it is more conducive to the growth of plants on the slope (Zhao et al. 2018). However, vegetation concrete is prone to collapse within 7d after spraying. At the same time, the durability of physical and mechanical indexes is also negatively affected under harsh conditions (Liu et al. 2013a, Gao et al. 2020). Therefore, it is significant to improve the initial stability and functional sustainability of vegetation concrete under harsh conditions.

Some studies have shown that the incorporation of fiber into the soil can effectively improve the shear strength, and tensile strength bearing capacity and enhance the toughness of soil (Wang et al. 2017, Li & Zornberg 2019, Zhao et al. 2021). And the cement soil reinforced by fibers has also concerned (Liang et al. 2016, Lu et al. 2016, Wang et al. 2018). The microscopic effect between cement and fiber was observed by SEM, Tang et al. (2011) and Yao et al. (2021) found that cohesion was the main force acting on the interface between cement and soil. At the same time, the increase of water content not only has no obvious effect on the bond strength, but it also can reduce the internal friction angle (Lovisa et al. 2010), therefore water content is also an important factor affecting fiber reinforcement. However, the internal friction angle of reinforced lime soil increased with the increase in curing time (Shi et al. 2011, Wang et al. 2019). And the incorporation of polypropylene fiber can improve the strength behavior of the material, and enhance the ductility and fracture toughness of the soil matrix (Liu

et al. 2013b). Therefore, it can be deduced that the polypropylene fiber was very appropriate to enhance the properties of vegetation concrete.

In this paper, a modified device was used to conduct a series of single fiber drawing experiments. The interfacial shear strength and the effect of water content, dry density, and curing time on the interfacial mechanical properties between polypropylene fiber and vegetation concrete were obtained. Finally, the drawing characteristics were analyzed and an empirical formula for the critical length of fiber was proposed, to guide the engineering application.

MATERIALS AND METHODS

Materials

The main materials required for the experiment include as follows: (1) Planting soil, which was taken from the common yellow-brown soil in Yichang City. It was air-dried and broken into pieces to pass through a 2 mm sieve. (2) P.O 42.5 ordinary Portland cement, which was produced by Huaxin Cement Co., LTD. (3) Organic material, which was prepared from local fir sawdust. (4) Amendment of habitat material, which was the patent product (Xu & Wang 2002) of China Three Gorges University. (5) Polypropylene fiber. (6) Water.

The composition and the physical properties of vegetation concrete are shown in Table 1 and Table 2. And the physical indexes of polypropylene fiber are listed in Table 3.

Preparation of Test Sample

As shown in Table 4, samples S_1~S_9 (1d curing time) were prepared with three ratios of water content and three ratios of dry density respectively. And samples T_1~T_9 (7d curing time) were prepared with the same method. The sample size is 5mm × 5mm × 5mm, and two small gaps (0.5 mm in width) were formed on the opposite sidewalls of the mold to facilitate fiber placement during compaction. The schematic diagram of the sample manufacture process is shown in Fig. 1, and the manufacturing method is described as follows:

(1) Half of the mixed material was put into the mold and flattened the surface carefully;

(2) Single polypropylene fiber was placed on the surface of the mixed material and passed through the reserved gap;

(3) The remaining half of the mixed material was put into the mold again and flattens the surface carefully;

(4) The piston was used to compact the mixed material to the target height;

(5) The sample was removed from the mold with the piston.

The samples were immediately wrapped with preservative film to prevent evaporation of water when manufacture was finished. At the same time, three parallel samples were prepared for taking the average value of the experiment.

Drawing Device and Testing Method

A device that was modified from the HP-50 HANDPI Digital Force Gauge was used in the test, as shown in Fig. 2. It was mainly composed of an HP-50 digital display drawing pressure gauge, tension sensor, drawing device, and other necessary instruments. The test method and operation process are introduced as follows:

(1) Place the sample in the left device in the figure, and pass the free section fiber at one end of the sample through the reserved joint of the left device;

(2) Fix the fiber of the free end with a modified HP-50 HANDPI Digital Force Gauge;

Table 1: Weight ratio of vegetation concrete.

Planting soil	Cement (P.O 42.5)	Organic material	Amendment of habitat material
100	10	6	4

Table 2: Basic physical property of vegetation concrete

Optimal water content	Plastic limit	Liquid limit	Maximum dry density
20%	19.5%	55%	1.99g/cm³

Table 3: Performance parameters of polypropylene fiber.

Diameter/ mm	Tensile strength/ MPa	Length/mm	Corrosion resistance
0.048	700	18	better

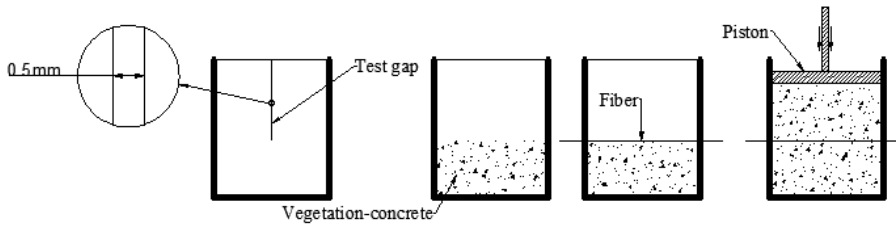

Fig. 1: Sketch drawing of sample prepared process.

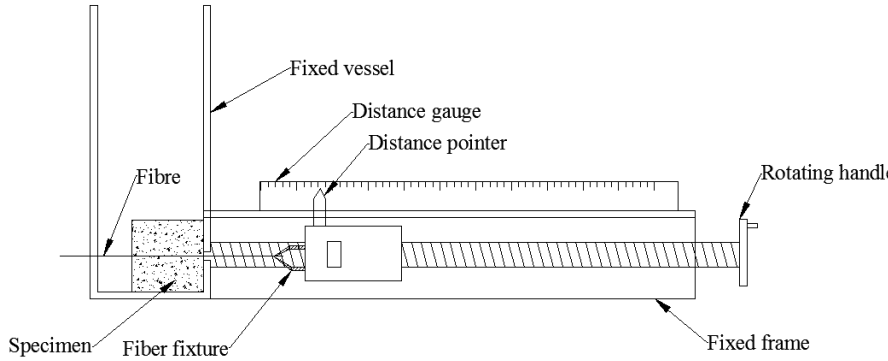

Fig. 2: Single fiber drawing test device.

(3) Connect the power supply to make the tension meter move uniformly at a constant speed of 1.5mm/min. At the same time, record the test process with the video device, finally, the indication number and displacement change of the tension meter were analyzed and extracted.

Ten data were continuously collected for the experiment required, and the experiment can be terminated when the variation range does not exceed 0.02N (Tang et al. 2009). Finally, the force in the final stable state was taken as the interfacial residual strength.

Computational Formula

The interfacial peak strength (*IPS*) and the interfacial residual strength (*IRS*) can be defined and calculated as follows (Zhang et al. 2015):

$$IPS = \frac{N_{max}}{S} \quad \ldots(1)$$

$$IRS = \frac{N_r}{S} \quad \ldots(2)$$

Where *IPS* is the interfacial peak strength (MPa); *IRS* is the interfacial residual strength (MPa); N_{max} is the peak load before the interfacial shear failure (N); *S* is the contact area between the fiber and vegetation concrete, which is calculated according to the size of the sample and the diameter of the fiber (mm^2); N_r is the residual tensile force when the tension meter value tends to be stable (N).

The critical length of fiber (l_c) can be calculated as follows (Tang et al. 2009):

$$l_c = \frac{R_f d}{2 \times IPS} \quad \ldots(3)$$

Where R_f is the tensile strength of the single fiber (MPa); *d* is the fiber diameter (mm); *IPS* is the interfacial peak strength (MPa).

Table 4: Test parameters of vegetation concrete.

Samples	Water content ω/%	Dry density [$g.cm^{-3}$]
S_1、T_1	18	1.7
S_2、T_2	18	1.8
S_3、T_3	18	1.9
S_4、T_4	20	1.7
S_5、T_5	20	1.8
S_6、T_6	20	1.9
S_7、T_7	22	1.7
S_8、T_8	22	1.8
S_9、T_9	22	1.9

RESULTS AND DISCUSSION

Drawing Characteristics of Single Fiber in Vegetation Concrete

As shown in Fig.3, it has a multi-peak characteristic of fiber-reinforced vegetation concrete. The tension increases and decreases repeatedly with the increase of displacement. And the tensile failure occurred when the tension tends to be stable gradually, then the load maintains a constant residual value until the end of the drawing test. According to the measured peak and residual drawing load, the corresponding interfacial peak strength (*IPS*) and interfacial residual strength (*IRS*)

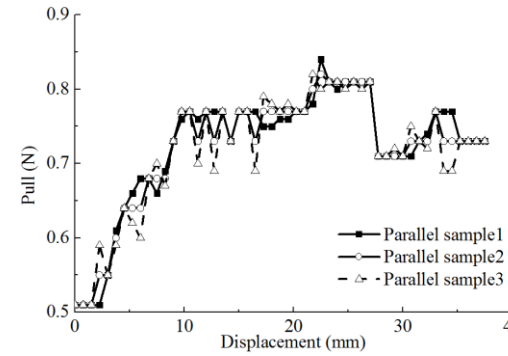

Fig. 3: Drawing curves of three parallel samples in S1.

are obtained. However, it has a single-peak characteristic of polypropylene fiber reinforced clay (Coppola et al. 2017, Van et al. 2019). Therefore, the difference between the drawing curves of clay and vegetation concrete is probably attributed to the different interface mechanical interactions.

The wave-like pattern of the drawing curves may be related to the cement hydration products in vegetation concrete. At the beginning of the experiment, the tensile force is not enough to deform the fiber, and the interface between the fiber and vegetation concrete slid with the increase of tensile force. The tensile force of the fiber is mainly linearly distributed during the separation process in clay (Gowthaman et al. 2018). However, the fiber is anchored by cement hydration products in vegetation concrete and produces relative motion by overcoming the anchoring force (Huang 2019). Due to the uneven distribution of cement hydration products in vegetation concrete, there are many anchoring sections on the fiber. Therefore, the drawing curve exhibits a multi-peak state distribution. Obviously, as the drawing displacement increases, the drawing load increases to overcome the anchoring of the first stage, then decreases, then increases when the next anchor is encountered, and then decreases again. After the fiber overcomes all anchoring forces, the fiber can only overcome the sliding friction. Due to the sliding friction being relatively stable, thus the interface residual strength and the range of variation are relatively stable.

The fibers were dyed with phenolphthalein after being stretched. The microscopic characteristic of dyed fibers before and after being drawn are shown in Fig.4 and analyzed as follows:

(1) The fiber diameter is significantly slender after the test. This is due to the plastic deformation of the fiber by tension, resulting in an increase in length but a gradual decrease in diameter.

(2) Many scratches appeared on the surface of the fiber. This indicates that the fiber is subjected to a force perpendicular to the fiber direction during stretching, which is extruded by hard particles in the vegetation concrete.

(3) There is a noticeable purple-red color in the fiber scratches and attachments after phenolphthalein dying, and only the cement hydration products are alkaline in the samples (Pan et al. 2020), which indicates that the main reason for the vertical force and cohesion is the existence of cement hydration products.

The Influence of Water Content

Water content has an important influence on *IPS* and *IRS* in vegetation concrete. As shown in Table 5, both *IPS* and *IRS* are minimal at the optimum water content (20%) in the 1d sample. The interfacial shear strength between the fiber and vegetation concrete is mainly composed of three parts: the anchoring force, interfacial friction force, and cohesion (Li et al. 2014). The anchoring force is mainly related to the content of cement, water, and cement hydration products. The interfacial friction is mainly related to particle shape, grain composition, normal stress, soil water content, and effective contact area with soil (Cai et al. 2006). In this study, the interfacial forces are the anchoring force and interfacial friction force. Due to the increase of water content in soil pores, the fiber has a certain lubricating effect when moving in the soil, thereby interfacial friction force decreased (Wu et al. 2012). The interfacial shear strength is lower at a water content of 20% than that of 18%. It is speculated that the cement hydration products in vegetation concrete are deficient when the water content is not reaching optimal, thus the increase rate of the anchoring force is slower than the interfacial friction force reduction rate.

The interfacial shear strength increases significantly at the water content of 22%. Reasons for that are the friction force becomes constant and the cement hydration products rapidly increase, resulting in the anchoring force increasing quickly with the increase of water content. When the water content exceeds the optimum water content, although the water between the particles becomes, even more, the excess free water promotes the hydration reaction of the cement, which increases the anchoring force, resulting in the interfacial friction force not continuing to decrease rapidly. Therefore, the increased range of anchoring force is higher than the decreased range of interfacial friction force, which results

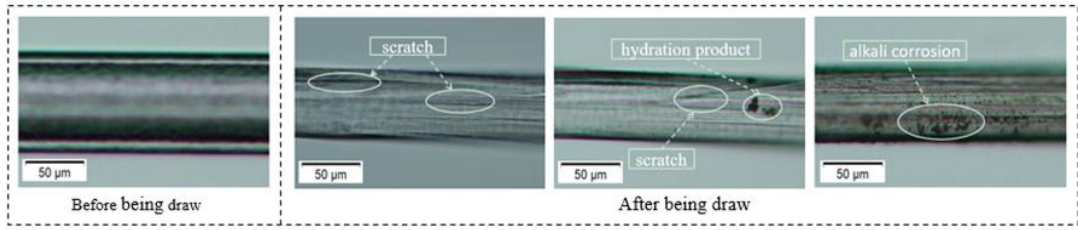

Fig. 4: Comparison of the fiber before and after being drawn.

Table 5: The results of *IPS* and *IRS* for vegetation concrete.

	Curing time/d	Water content/%	Interfacial shear strength/(MPa)		
			1.7 g.cm^{-3}	1.8 g.cm^{-3}	1.9 g.cm^{-3}
IPS	1	18	0.82	0.94	0.98
		20	0.77	0.87	0.98
		22	0.86	0.99	1.03
	7	18	0.86	0.77	1.11
		20	0.96	1.26	1.28
		22	0.96	1.31	1.32
IRS	1	18	0.73	0.9	0.9
		20	0.71	0.8	0.9
		22	0.81	0.9	0.99
	7	18	0.77	0.68	1.03
		20	0.81	1.01	1.07
		22	0.9	1.01	1.12

in a corresponding increase of interfacial shear strength at a water content of 22%. As shown in Table 5, there are some differences between the curing time of 1d and 7d. As the curing time increases, the degree of cement hydration reaction is more intense, and more cement hydration products are produced, resulting in the interfacial shear strength at the water content of 20% being higher than that of 18%. It can be seen from Fig.5, that the drawing curves still show multi-peak characteristics at different water content, which indicates that the water content has no significant influence on the drawing curve characteristic.

The Influence of Curing Time

As shown in Table 5, as the curing time increases, the increased range of *IPS* is 4.88%~44.83% and the increased range of *IRS* is 5.48%~26.25%. The reason for that is the cement hydration products are even more and the particles are larger in the 7d sample (Ruan et al. 2016). Thus, the cement hydration products and fiber have more anchoring points, which enhance the anchoring force between the fiber and vegetation concrete. The microstructure of cement under different curing times is different, and the flocculation and hydration products appear in the process of cement hydration reaction gradually (Wang et al. 2008). These products attach to the interface of the fiber and then reinforce the interface between the fiber and vegetation concrete. Besides, as the curing time increases, the cement hydration products fill the pores of soil particles. Therefore, the effective contact area between the fiber and vegetation concrete is increased, and the interfacial shear strength between the fiber and vegetation concrete is further enhanced.

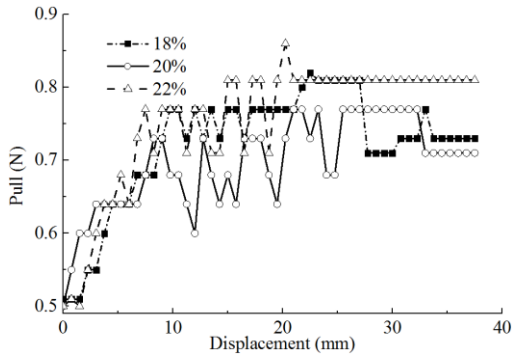

Fig. 5: Drawing curves of 1d samples in the dry density of 1.7 g/cm^3.

The Influence of Dry Density

As shown in Fig. 6, with the increase in dry density, the *IPS* and *IRS* increase by 27.27% and 11.11% respectively. As the dry density increases, the effective contact area between the fiber and hard particles increases accordingly, and the corresponding vertical stress which is acting on the fiber by cement hydration products also increases, thus enhancing the anchoring force among the interface of vegetation concrete. For vegetation concrete with different dry densities, the increase of dry density also reduces the porosity among the particles of vegetation concrete (Zhao et al. 2013). The effective contact area increases relatively between the fiber and vegetation concrete, and the interfacial friction force between the fiber and vegetation concrete also increases (Zhang et al. 2014). Moreover, the increases in dry density result in the fiber extruded by hard particles in vegetation concrete, which causes the fiber in the sample to bend, thus increasing the effective contact area between the fiber and

vegetation concrete, and increasing the interfacial friction force.

The Determination of the Critical Length and Empirical Formula

Determination of the Critical Length

Determining the reasonable length of the fiber is significant in practical engineering. If the length of the actual fiber is short than the critical length, the incorporated fiber is pulled out when vegetation concrete is destroyed (Liang et al. 2016); when the fiber length exceeds the critical length, the fiber breaks in the middle position and cause fiber waste (Zhao et al. 2015); however, the fiber deformed firstly when the length of the fiber equal to the critical length, then the middle of the fiber will gradually become thinner until it is broken. Therefore, the critical length is a key factor to maximize the mechanical properties of polypropylene fiber when it is used as reinforced material in engineering. To calculate the critical length of polypropylene fiber, the assumptions were made as follows:

(1) The direction of the fiber is always consistent with the tensile meter;

(2) The interfacial shear strength of vegetation concrete remains constant during the drawing process.

Therefore, the maximum critical length of the fiber-reinforced vegetation concrete proposed in this study is a reference for the design of practical projects. The maximum critical length of the fiber is calculated by the formula (3) and the results are shown in Table 6.

Determination of Empirical Formula

(1) Establish an empirical formula

It is observed from Table 6, that with the increase in curing time, the interfacial peak strength (*IPS*) between vegetation concrete and the fiber increases, and the critical length of fiber decreases. The interfacial shear strength of vegetation concrete has a low power at the initial stage of spraying. Therefore, adding the appropriate length of fiber at this stage can effectively improve engineering strength. In this study, the maximum critical length (l_{max} *The*) the empirical formula only includes the water content (ω), the dry density (ρ), and the curing time (T) of the vegetation concrete. It is introduced and defined as follows:

$$l_{max} = k\omega^a \rho^b T^c \quad \ldots(4)$$

Where l_{max} is the critical length of the fiber (mm); ω is the water content (%); ρ is the dry density (g.cm^{3-}); is the curing time (d); k、 a、 b and c are constants in the empirical formula. It should be explained that the empirical formula does not take into account the difference between the left and right dimensions of the equation. The purpose is only to give a numerical empirical formula.

The logarithmic equation is drawn from the logarithm of the left and right sides of equation (4) as follows:

$$lgl_{max} = lgk + alg\omega + blg\rho + clgT \quad \ldots(5)$$

Established $Y = lgl_{max}$, $m = lgk$, $X_1 = lg\omega$, $X_2 = lg\rho$, $X_3 = lgT$ and get the transformation of multivariate regression linear equation as follows:

$$Y = m + aX_1 + bX_2 + cX_3 \quad \ldots(6)$$

The experimental data of S_1-S_9 were substituted into the formula (6), and the unknown coefficients *m, a, b,* and *c* of the multiple linear regression equation can be solved.

(2) Empirical formula

The multiple linear regression equation was solved by the experimental data. As shown in Fig. 7, the experimental data indicates that the independent variable correlation is not obvious. Moreover, the R^2 of the model is 0.72 and the correlation is remarkable (p<0.05) indicating that the model design is reasonable.

Consequently, the results of the four unknown coefficients in equation (6) are obtained: m= 2.746, a= -0.804,

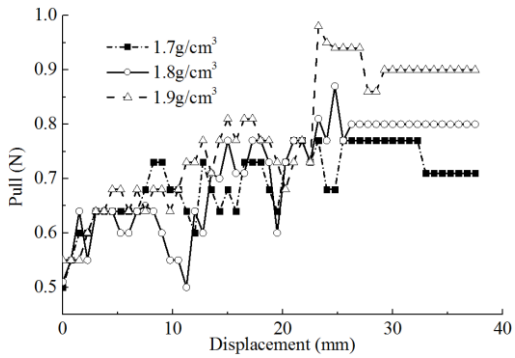

Fig. 6: Drawing curves of 1d samples in water content of 20%.

Table 6: Results of the critical length for all samples.

Samples	mm	Samples	mm
S_1	15.45	T_1	14.73
S_2	13.48	T_2	16.45
S_3	12.93	T_3	11.41
S_4	16.45	T_4	13.20
S_5	14.56	T_5	10.05
S_6	12.93	T_6	9.90
S_7	14.73	T_7	13.20
S_8	12.80	T_8	9.67
S_9	12.30	T_9	9.59

b= 2.194 and c= -0.084. Thus, the equation is expressed as follows:

$$Y = 2.746 - 0.804X_1 - 2.194X_2 - 0.084X_3 \quad \ldots(7)$$

Substituted $Y= lgl_{max}$, $m= lgk$, $X_1= lg\omega$, $X_2= lg\rho$, and $X_3= lgT$ to formula (7) and converted as follows:

$$lgl_{max} = 2.746 - 0.804lg\omega - 2.194lg\rho - 0.084lgT \quad \ldots(8)$$

The equation on both sides of equation (8) was logarithmic, and then the equation is converted as follows:

$$l_{\max} = 10^{2.746}\omega^{-0.804}\rho^{-2.1941}T^{-0.084} \quad \ldots(9)$$

Therefore, formula (9) can be confirmed as the empirical formula for the maximum critical length of polypropylene fiber in vegetation concrete from 1d curing time to 7d curing time.

CONCLUSION

(1) The drawing curves of polypropylene fiber and vegetation concrete showed a typical multi-peak characteristic. And as the curing time increases, the increased range of *IPS* is 4.88%~44.83% and the increased range of *IRS* is 5.48%~26.25%.

(2) The strength of cement hydration products increases with the increase of curing time, thus the anchoring force between vegetation concrete and the fiber is improved. The interfacial shear strength is the minimum at the optimum water content (20%) in the 1d sample. In addition, the *IPS* and *IRS* increase with the increase of dry density.

(3) The empirical formula of the critical length is obtained by multiple linear regression analysis and combined with mathematical calculation. The formula will provide a reference for the suitable deployment of polypropylene fiber length in vegetation concrete under different design and engineering conditions.

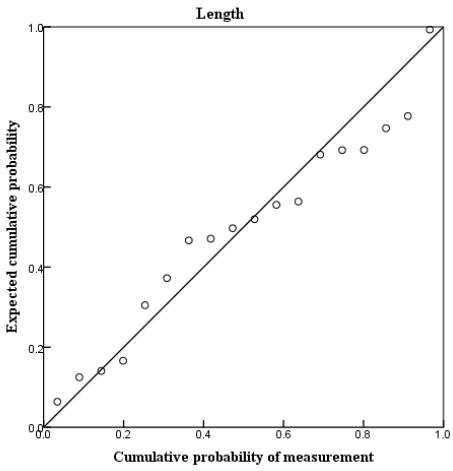

Fig. 7: Normal P-P graph of regression normalized residual.

ACKNOWLEDGEMENTS

This study was supported by the National Key R&D Program of China (Grant No. 2017YFC0504902-02), the National Natural Science Foundation of the People's Republic of China (Grant No. 51708333), the Natural Science Foundation of Hubei Province (Grant No. 2020CFB317), the CRSRI Open Research Program (Grant No. CKWV2019753/KY), the Open Fund of Key Laboratory of Mountain Hazards and Surface Processes, Chinese Academy of Sciences (Grant No. 2019001), the Research Fund for Excellent Dissertation of China Three Gorges University (Grant No. 2021SSPY018).

REFERENCES

Cai, Y., Shi, B., Ng, C.W.W. and Tang, C.S. 2006. Effect of polypropylene fiber and lime admixture on engineering properties of clayey soil. Eng. Geol., 87(3-4): 230-240.

Coppola, B., Scarfato, P., Incarnato, L. and Di Maio, L. 2017. Morphology development and mechanical properties variation during cold-drawing of polyethylene-clay nanocomposite fibers. Polymers, 9(6): 1-17.

Gao, J.Z., Zhou, M.T., Xu, W.N., Liu, D.X., Shen, J. and Peng, S.T. 2020. The evolution of structural properties of vegetation concrete under freeze-thaw cycles. Int. J. Elect. Eng., 29: 61 doi: 10.1177/0020720920930363.

Gowthaman, S., Nakashima, K. and Kawasaki, S. 2018. A state-of-the-art review on soil reinforcement technology using natural plant fiber materials: Past findings, present trends, and future directions. Materials, 11(4): 553.

Huang, M.J. 2019. Experimental study on split tensile strength of glass fiber reinforced cement soil. J. Rail. Sci. Eng., 16(4): 938-942.

Li, C.L. and Zornberg, J.G. 2019. Shear strength behavior of soils reinforced with weak fibers. J. Geotech. Geoenviron. Eng., 145(9): 06019006.

Li, J., Tang, C.S., Wang, D.Y., Shi, B. and Pei, X.J. 2014. Study on the interfacial shear strength of wave-shape fiber reinforced soil through single fiber pullout tests. Chinese J. Geotech. Eng., 36(9): 1696-1704.

Liang, Y.Z., Chen, Y., Liu, D.X., Xu, W.N. and Yao, X.Y. 2016. Effect of additive plant fiber on shearing strength of vegetation-compatible concrete under freezing-thawing cycles. Bull. Soil Water Conserv., 36(2): 136-139+145.

Liu, B.S., Tang, C.S., Li, J., Wang, D.Y., Zhu, K. and Tang, W. 2013b. Advances in engineering properties of fiber-reinforced soil. J. Eng. Geol., 21(4): 540-547.

Liu, D.X, Xu, W.N., Cheng, Z.L., Zhou, Z.J. and Cai, X.Y. 2013a. Improvement test on frost resistance of vegetation-concrete and engineering application of test fruitage. Environ. Earth Sci., 69(1): 161-170.

Lovisa, J., Shukla, S.K. and Sivakugan, N. 2010. Shear strength of randomly distributed moist fiber-reinforced sand. Geosynth. Int., 17(2): 100-106.

Lu, Q., Guo, S.L., Wang, M.M. and Gao, M. 2016. Experimental study of mechanical properties of fiber cement soil. Rock Soil Mech., 37(2): 421-426.

Pan, B., Ding, Y., Huang, X.L., Gao, F., Xu, W.N. and Liu, D.X. 2020. Study on mechanical properties of fiber-reinforced vegetation concrete under dry and wet cycle. J. China Three Gorges Univ. Nat. Sci., 42(1): 63-67.

Ruan, B., Peng, X.X. and Deng, L.F. 2016. Experimental study on shear strength parameters of cement-soil. J. Rail. Sci. Eng., 13(4): 662-668.

Shi, L.G., Zhang, M.X. and Cao, P. 2011. Triaxial shear strength characteristics of lime-soil reinforced with polypropylene fiber inclusions. Rock Soil Mech., 32(9): 2721-2728.

Tang, C.S., Shi, B. and Gu, K. 2011. Microstructural study on interfacial interactions between fiber reinforcement and soil. J. Eng. Geol., 9(4): 610-614.

Tang, C.S., Shi, B., Gao, W. and Liu, J. 2009. Single fiber pull-out test and the determination of critical fiber reinforcement length for fiber-reinforced soil. Rock Soil Mech., 30(8): 2225-2230.

Van, T.B., Reynolds, C.T., Bilotti, E. and Peijs, T. 2019. Nanoclay assisted ultra-drawing of polypropylene tapes. Nanocomposites, 5(4): 114-123.

Wang, B., Yang, W.M. and Li, Z.Q. 2008. Micro mechanism of strength increase with curing time for compacted cement soil. J. Univ. Sci. Technol. Beij, 30(3): 233-238.

Wang, M.M., Lu, Q., Guo, S.L., Gao, M. and Shen, Z.T. 2018. Dynamic behavior of soil with fiber and cement under cyclic loading. Rock Soil Mech., 39(5): 1753-1760.

Wang, Y.X., Guo, P.P., Li, X., Lin, H., Liu, Y. and Yuan, H.P. 2019. The behavior of fiber-reinforced and lime-stabilized clayey soil in triaxial tests. Appl. Sci. Basel, 9(5): 900.

Wang, Y.X., Guo, P.P., Ren, W.X., Yuan, B.X., Yuan, H.P. and Zhao, Y.L. 2017. Laboratory investigation on strength characteristics of expansive soil treated with jute fiber reinforcement. Int. J. Geomech., 17(11): 04017101.

Wu, Y.K., Niu, B. and Sang, X.S. 2012. Experimental study of mechanical properties of soil randomly included with sisal fiber. Hydrogeol. Eng. Geol., 39(6): 77-81.

Xia, Z.Y., Xu, W.N. and Wang, L.H. 2011. Research on characteristics of early strength of ecological slope-protected base material of vegetation-growing concrete. Rock Soil Mech., 32(6): 1719-1724.

Xu, W.N., Xia, D., Zhao, B.Q., Xia, Z.Y., Liu, D.X. and Zhou, M.T. 2019. Research on Vegetation Ecological Restoration Technology in Disturbed Areas Of Hydropower Projects. Science Press, Beijing, pp. 108-113.

Yao, X., Huang, G., Wang, M.M. and Dong, X.Q. 2021. Mechanical properties and microstructure of PVA fiber-reinforced cemented soil. KSCE J. Civil Eng., 25(2): 482-491.

Zhang, C.C., Zhu, H.H., Tang, C.S. and Shi, B. 2015. Modeling of progressive interface failure of fiber-reinforced soil. J. Zhejiang Univ. Eng. Sci., 49(10): 1952-1959.

Zhao, B.Q, Xia, L., Xia, D., Liu, D.X. and Xia, Z.Y. 2018. Effect of cement content in vegetation concrete on soil physico-chemical properties, enzyme activities, and microbial biomass. Nat. Environ. Pollut. Technol., 17(4): 1065-1075.

Zhao, C., Shen, X.D., Jia, S.H. and Zhao, C.F. 2013. Influence of density on strength of cemented soil. Chin. J. Geotech. Eng., 35(S1): 360-365.

Zhao, N.Y., Wu, H.J. and Huang, Z.Y. 2021. Strength behavior of red clay reinforced by basalt chopped fiber. Arab. J. Geosci., 14(1): 15.

Zhao, Y.P., Yan, H. and Han, J. 2015. Analysis of the macroscopic interfacial behavior of the fiber pullout using an elastic-plastic cohesive model. Chin. J. Theoretical Appl. Mech., 47(1): 127-134.